Localization of the Retinal Protonated Schiff Base Counterion in Rhodopsin

May Han, Brian S. DeDecker, and Steven O. Smith
Department of Molecular Biophysics and Biochemistry, Yale University, New Haven, Connecticut 06511 USA

ABSTRACT Semiempirical molecular orbital calculations are combined with ^{13}C NMR chemical shifts to localize the counterion in the retinal binding site of vertebrate rhodopsin. Charge densities along the polyene chain are calculated for an 11-*cis*-retinylidene protonated Schiff base (11-*cis*-RPSB) chromophore with 1) a chloride counterion at various distances from the Schiff base nitrogen, 2) one or two chloride counterions at different positions along the retinal chain from C_{10} to C_{15} and at the Schiff base nitrogen, and 3) a carboxylate counterion out of the retinal plane near C_{12}. Increasing the distance of the negative counterion from the Schiff base results in an enhancement of alternating negative and positive partial charge on the even- and odd-numbered carbons, respectively, when compared to the 11-*cis*-RPSB chloride model compound. In contrast, the observed ^{13}C NMR data of rhodopsin exhibit downfield chemical shifts from C_8 to C_{13} relative to the 11-*cis*-RPSB·Cl corresponding to a net increase of partial positive or decrease of partial negative charge at these positions (Smith, S. O., I. Palings, M. E. Miley, J. Courtin, H. de Groot, J. Lugtenburg, R. A. Mathies, and R. G. Griffin. 1990. *Biochemistry.* 29:8158–8164). The anomalous changes in charge density reflected in the rhodopsin NMR chemical shifts can be qualitatively modeled by placing a single negative charge above C_{12}. The calculated fit improves when a carboxylate counterion is used to model the retinal binding site. Inclusion of water in the model does not alter the fit to the NMR data, although it is consistent with observations based on other methods. These data constrain the location and the orientation of the Glu^{113} side chain, which is known to be the counterion in rhodopsin, and argue for a strong interaction centered at C_{12} of the retinylidene chain.

INTRODUCTION

Visual pigments absorb light over a wide range of wavelengths (Nathans, 1992). The absorption maximum of vertebrate rod pigments is ~500 nm, while it varies from 420 to 610 nm in cone pigments. The photoreactive chromophore in these proteins is 11-*cis*-retinal covalently attached to a lysine side chain through a protonated Schiff base (PSB) linkage. One of the intriguing questions in the area of visual photochemistry has been how the protein in rod and cone pigments modulates the absorption spectrum of the 11-*cis* retinylidene chromophore to generate pigments of different colors.

Several models have been proposed for the chromophore-protein interactions that are responsible for the spectral tuning of visual pigments. A common element of each model is that increased delocalization of the conjugated π electrons along the retinylidene chain leads to a red-shift in the chromophore's absorption maximum. Protonation of a retinylidene Schiff base adds a net positive charge to the conjugated system that can be localized to the Schiff base linkage by close association of a negative counterion. Charge delocalization leading to spectral red-shifts may result from simply increasing the separation between the PSB and its associated counterion (Blatz et al., 1972) or from placing charged or polar residues along the conjugated chain that stabilize partial positive charge on the retinal carbons away from the PSB (Kropf and Hubbard, 1958; Honig et al., 1976). Based on absorption spectra of rhodopsin regenerated with dihydroretinals, Honig et al. (1979) argued that the chromophore interacts with two negative charges in its protein binding site. One charge acts as a counterion to the PSB, while a second charge situated between C_{12} and C_{14} of the retinal generates a red-shift in the chromophore's absorption band. Birge and coworkers have proposed that a single charge interacts with the retinylidene chromophore in rhodopsin on the basis of two-photon absorption studies indicating a neutral retinal binding site (Birge et al., 1985). They modeled the retinal binding site with a carboxylate counterion interacting primarily with C_{13} and C_{15}, without excluding the possibility of it being closer to the center of the polyene chain, and argued that the imine proton hydrogen bonds to water rather than directly to the counterion (Birge et al., 1988; Birge, 1990; Tallent et al., 1992). Recently, several groups using site-directed mutagenesis of charged residues in rhodopsin have shown that glutamate 113 serves as the counterion in the retinal binding site (Zhukovsky and Oprian, 1989; Sakmar et al., 1989; Nathans, 1990), although its location and orientation relative to the retinylidene chromophore are still not well-established.

We have been addressing the question of counterion location in both rhodopsin and its photointermediates using ^{13}C-magic angle spinning NMR (Smith et al., 1990; Smith et al., 1991). The ^{13}C chemical shift is sensitive to the electron density surrounding the carbon nucleus and provides a

Received for publication 25 January 1993 and in final form 23 April 1993.
Address reprint requests to Steven O. Smith at the Department of Molecular Biophysics and Biochemistry, Yale University, 260 Whitney Ave., New Haven, CT 06511. Tel.: 203-432-5095.

Abbreviations used: CNDO, complete neglect of differential overlap; INDO, intermediate neglect of differential overlap; MNDO, modified neglect of diatomic overlap; PSB, protonated Schiff base; 11-*cis*-RPSB, 11-*cis*-N-retinylidene protonated Schiff base; 11-*cis*-RSB, 11-*cis* unprotonated retinylidene Schiff base; ZDO, zero differential overlap.

0006-3495/93/08/899/08 $2.00

probe of the partial charge on each carbon of the conjugated retinal chain. It has been shown that the ^{13}C chemical shift has a linear relationship with the charge density in conjugated systems and exhibits a correlation of approximately −160 ppm/electron or 160 ppm/unit charge, where unit charge represents the magnitude of the electron charge (Spiesecke and Schneider, 1961). By comparing the retinal ^{13}C chemical shifts between model compounds and rhodopsin, it has been possible to characterize how the charge density at each position of the retinylidene PSB *changes* between solution and the protein binding site. We have previously observed a large (6.2 ppm) change in the ^{13}C chemical shift at position 13 of rhodopsin relative to the 11-*cis*-*N*-retinylidene-*n*-propyliminium chloride (11-*cis*-RPSB·Cl) model compound (Smith et al., 1990). The downfield shift at C_{13} is correlated with an increase of partial positive charge and has been used to support the idea of a negative protein counterion located near this position (Smith et al., 1990). However, extensive model compound studies indicate that a large downfield chemical shift of C_{13} can arise from changes in either the nature of the counterion or solvent environment, whereas C_{12} and other even-numbered carbons are extremely insensitive to such changes (Albeck et al., 1992). Interestingly, each of the retinal carbons from C_8 to C_{13} in rhodopsin exhibits an increase in partial positive charge relative to the 11-*cis*-RPSB·Cl reference compound. As a result, it is necessary to correlate the changes in charge density along the *entire* conjugated retinal chain. An alternation of charge density difference is often observed between odd- and even-numbered carbon atoms when model systems are compared (Shriver et al., 1976, 1979; Harbison et al., 1985; Albeck et al., 1992), suggesting that the anomalous pattern observed in the rhodopsin NMR data may lead to a unique solution for the location of the counterion.

Semiempirical electronic calculations have been used extensively to model how the electron densities along the retinylidene chain change with chromophore structure and environment (Warshel and Karplus, 1974; Tavan et al., 1985; Rodman Gilson and Honig, 1988; Tallent et al., 1992). These studies have yielded insights into the ground and excited states of the retinal molecule and have provided useful qualitative and quantitative information for interpreting absorption and NMR measurements. In this communication, semiempirical calculations are combined with experimental ^{13}C NMR chemical shifts to address the question of counterion location in vertebrate rhodopsin. A great advantage of NMR over previous methods used to localize the rhodopsin counterion arises from the availability of *local* charge density information at each conjugated carbon atom in addition to *global* information obtained from the pattern of charge density variation along the retinylidene chain.

METHODS

A linear relationship between chemical shift and electron density for conjugated systems has been observed by several groups with a correlation of approximately 160 ppm/unit charge. The correlation is derived from the observed chemical shift and electron densities based on either the symmetry of the molecule (Spiesecke and Schneider, 1961) or semiempirical calculations (Lauterbur, 1961; Tokuhiro and Fraenkel, 1969). The latter results depend in part on the method of calculation. Tokuhiro and Fraenkel (1969) obtained their best linear correlations (155 ppm/unit charge) when both π and σ electrons were included in the calculated charge densities. The linear correlation improves when charge density and chemical shift *differences* are considered instead of their absolute value (Rodman Gilson and Honig, 1988). These studies suggest that *changes* in observed chemical shifts might be modeled both qualitatively and quantitatively by electronic calculations.

Fig. 1 *a* shows the structure of the retinylidene PSB cation used for the model compound and rhodopsin calculations. The 11-*cis*-RPSB geometry was energy-minimized using the MOPAC program (M. J. S. Dewar, University of Texas, Austin) with the MNDO Hamiltonian while holding the C_6-C_7 and C_{12}-C_{13} torsion angles at 45° and 40°, respectively (Honig and Karplus, 1971; Gilardi et al., 1972; Birge et al., 1988). Charge densities were calculated using both the zero-differential overlap (ZDO) and intermediate neglect of differential overlap (INDO) approximations with the ZINDO program (M. Zerner, Florida State University). The qualitative fits of the calculated charge densities to the experimental data are very similar, and the conclusions drawn are the same for both methods. The data presented in this study are the results using the ZDO approximation. The counterions used in the calculations are either full charges (such as Cl^- and Br^-) or a group of partial charges, such as CH_3-COO^- and H_2O, whose charge distributions are obtained from separate calculations of the individual groups.

Rodman Gilson and Honig (1988) have shown that good correlations can be obtained between the observed chemical shift and calculated charge density *differences* in retinal systems using CNDO calculations. We have taken a similar approach and use the 11-*cis*-RPSB·Cl model compound in a hydrophobic environment as a reference to avoid complications in modeling polar solvent interactions. The ^{13}C chemical shifts of 11-*cis*-RPSB·Cl obtained in $CDCl_3$ are listed in Table 1. The data presented below are all differences relative to this model compound. In determining the charge densities for the 11-*cis*-RPSB·Cl, the chloride counterion was positioned 3.25 Å away from the Schiff base nitrogen along the N-H bond based on the crystal structures of related compounds (Blatz et al., 1972; Zelnik et al. 1986).

In order to test the approach described above, we have calculated the charge density differences between two 11-*cis*-retinal model compounds and the reference 11-*cis*-RPSB·Cl. The first model compound comparison is with the 11-*cis* unprotonated retinylidene Schiff base (11-*cis*-RSB). The 11-*cis*-RSB is neutral and consequently it is not necessary to define a counterion location. The plot of charge density difference as a function of each conjugated carbon position along the retinal chain is shown in Fig. 1 *b*. The experimental charge density differences were obtained from the observed differences in chemical shift (Table 1) divided by the 160-ppm/unit-charge correlation discussed above. An alternation in charge differences is observed and is qualitatively fit by the calculation as one proceeds along the chain from C_{15} to C_5. The quantitative fit of the experimental data is evaluated by the linear correlation between the observed chemical shift difference and the calculated charge density difference (Fig. 1 *c*). A perfect fit would have a slope of 160 ppm/unit charge, a Y intercept of 0, and a correlation coefficient (R) of 1. Acceptable fits in this study were those that had correlation coefficients greater than 0.80, slopes between 90 and 250 ppm/unit charge, and intercepts less than 1.0 ppm. In Fig. 1 *c*, a good correlation is obtained with a high correlation coefficient of 0.98, a slope of 212 ppm/unit charge, and an intercept of 0.69 ppm if C_{15} is excluded from the linear fit. Deviation of the calculated value for C_{15} has also been seen using Pariser-Parr-Pople (Shriver et al., 1976) and CNDO (Inoue et al., 1977) calculations and may result from poor parameterization of the Schiff base linkage. Consequently, C_{15} has not been used in this study for quantitation of the calculated fits to the experimental data.

The second comparison is between the 11-*cis*-RPSB·Br model compound and the 11-*cis*-RPSB·Cl reference. Since bromide and chloride differ mainly in their van der Waals radii, the changes in charge density can be readily modeled by a small change (0.15 Å) in the location of the center of the counterion relative to the SB nitrogen (Blatz et al., 1972; Sanders et al. 1983). As in the 11-*cis*-RSB comparison, an alternation in charge differences is observed along the retinal chain, and the calculated differences agree both

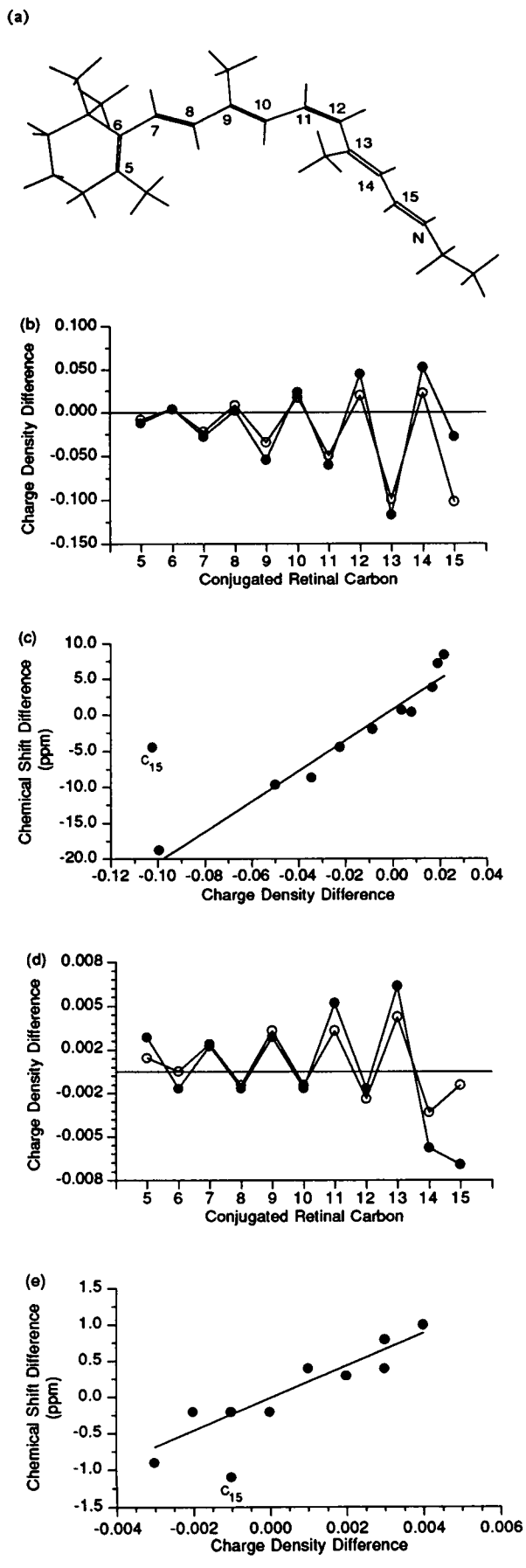

TABLE 1 ^{13}C chemical shifts (ppm) for rhodopsin and retinylidene model compounds

Carbon	Rhodopsin[a]	11-*cis*-RPSB·Cl[b]	11-*cis*-RPSB·Br	11-*cis*-RSB[b]
C_5	130.3 ppm	131.7	132.1	129.7
C_6	137.7	137.2	137.0[c]	137.5
C_7	132.3	132.3	132.6	127.8
C_8	139.2	137.2	137.0[c]	138.0
C_9	148.5	146.6	147.0	139.3
C_{10}	127.8	126.4	126.2	126.3
C_{11}	141.6	137.5	138.3	127.7
C_{12}	132.1	129.0	128.8	131.7
C_{13}	168.9	162.7	163.7	145.0
C_{14}	121.2	121.3	120.4	130.0
C_{15}	165.4	163.9	162.8	159.6

Model compound data were obtained in $CDCl_3$. Chemical shifts are referenced to TMS.

[a] Smith et al. (1990).

[b] Shriver et al. (1979).

[c] Not resolved.

qualitatively and quantitatively ($R = 0.95$) with the experimental data (Fig. 1, *d* and *e*). A similar plot was obtained for the differences between the all-*trans* bromide and chloride retinylidene PSBs in the solid state (Harbison et al., 1985). The chemical shift differences observed in rhodopsin (≤6.2 ppm) fall between the large changes observed for the 11-*cis*-RSB and 11-*cis*-RPSB·Cl comparison (up to 17.7 ppm) and the much smaller changes for the 11-*cis*-RPSB·Br and 11-*cis*-RPSB·Cl comparison (≤1.0 ppm). The agreement between the calculated fits and the experimental data for these two extremes argues that the electron density changes in rhodopsin can be modeled using these ground-state calculations.

Solution ^{13}C NMR spectra of the 11-*cis*-RPSB·Br model compound were obtained in $CDCl_3$ at −30°C to prevent isomerization. Spectral assignments were made by comparison with the 11-*cis*-RPSB·Cl (Shriver et al., 1979) and the 11-*cis*-retinylidene-*n*-*tert*-butyliminium perchlorate (Smith et al., 1990) model compounds. The Schiff base was prepared with propylamine in diethylether and protonated with HBr using modified procedures of Blatz et al. (1972) and Shriver et al. (1979).

RESULTS

There are several specific models for how the opsin interacts with the chromophore in visual pigments that can be tested by comparing predicted charge distributions with experimental charge densities obtained from ^{13}C chemical shifts. In order to test these models and further localize the counterion, we first characterize how the charge density changes due to charge separation between the PSB and a negative counterion. We then systematically move a single chloride counterion along the retinal chain and compare the calculated

FIGURE 1 11-*cis*-RPSB structure and model compound calculations. (*a*) The structure of the 11-*cis*-RPSB with ethylamine forming the SB linkage. (*b*) Comparison of the calculated (○) and experimental (●) charge density differences of the 11-*cis*-RSB relative to the 11-*cis*-RPSB·Cl reference. (*c*) Correlation of the experimental chemical shift difference and the calculated charge density difference of the 11-*cis*-RSB. The linear fit yields a slope of 212 ppm/unit charge, an intercept of 0.69 ppm and a correlation coefficient of 0.98. C_{15} is not included in the linear fit. (*d*) same as (*b*), except the model compound used is 11-*cis*-RPSB·Br. (*e*) same as (*c*) except the compound is 11-*cis*-RPSB·Br and the fit yields a slope of 226 ppm/unit charge, an intercept −0.02 ppm and an R of 0.95. Note the difference in the scale in (*b*) and (*d*).

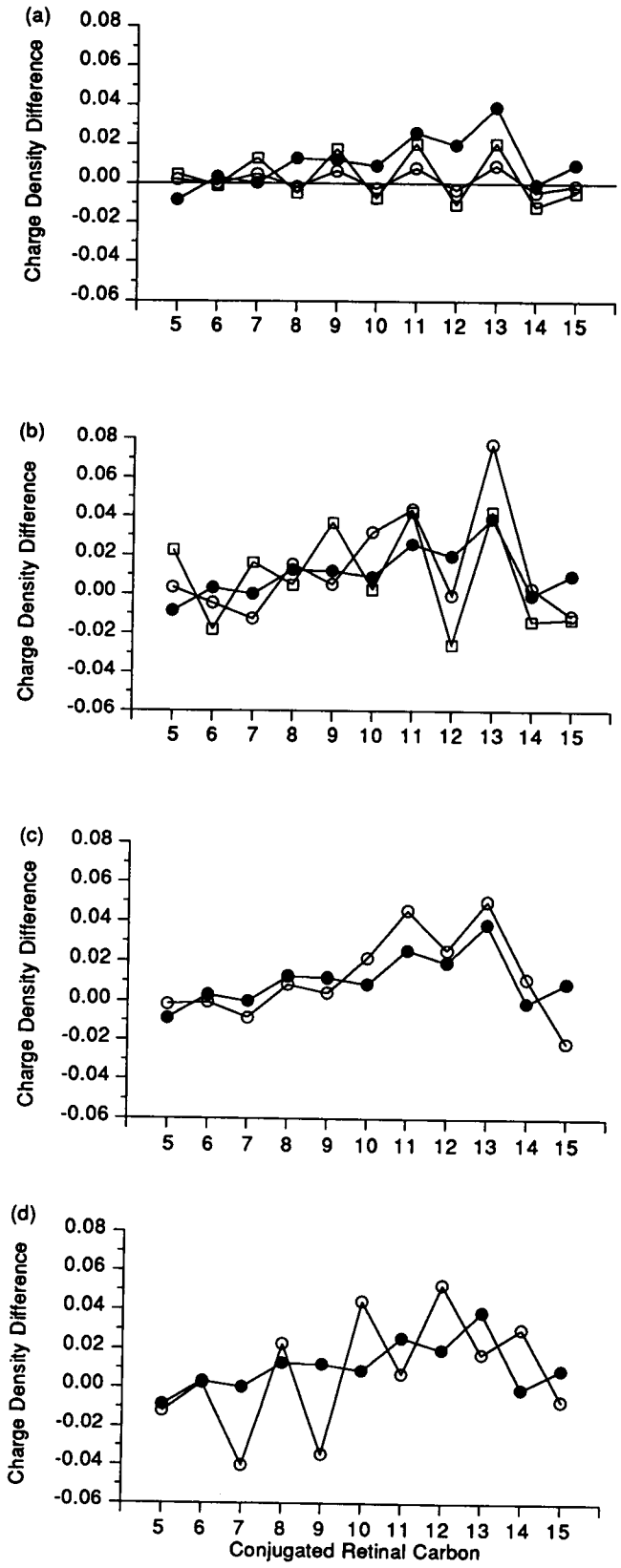

FIGURE 2 Modeling the retinal binding site of rhodopsin with chloride counterions. In each plot the experimental charge density differences for rhodopsin relative to the 11-*cis*-RPSB·Cl reference are given by the filled symbols. (*a*) Calculated charge density differences relative to 11-cis-RPSB·Cl with a chloride ion at 4.0 Å (○) and 6.0 Å (□) from the Schiff base nitrogen along the N-H bond. (*b*) Calculated charge density differences with a chloride ion at 3.0 Å (○) and 5.0 Å (□) from C_{13} with the $C_{13}\cdots Cl^-$ axis perpendicular to the RPSB plane. (*c*) Calculated charge density differences with a chloride ion at 3.0 Å from C_{12} with the $C_{12}\cdots Cl^-$ axis perpendicular to the RPSB plane (○). (*d*) Calculated charge density difference with one chloride ion as in (*c*) and a second chloride at 3.25 Å from the nitrogen along the N-H bond.

changes in charge density with the experimental data. The calculations are repeated for selected orientations with two chloride counterions. Finally, a carboxylate counterion is used to model the Glu^{113} side chain which is known to serve as the counterion to the rhodopsin chromophore.

Blatz and coworkers (1972) proposed that visual pigments modulate their absorption spectra by varying the distance between negative and positive charge. One way that this can be tested is by increasing the separation between the positively charged Schiff base and an associated negative counterion. Fig. 2 *a* (*open symbols*) shows how the charge density changes on the retinylidene carbons due to increased charge separation. The calculations are for 11-*cis*-RPSB models with a chloride counterion at 4.0 Å (*open circles*) and 6.0 Å (*open squares*) from the PSB nitrogen along the N-H bond. The differences, as mentioned above, are relative to the reference 11-*cis*-RPSB with a chloride counterion at 3.25 Å. It is worth emphasizing that even though the charge density *difference* at each conjugated carbon can be positive or negative depending on the counterion model, the absolute partial charges are always negative on the even-numbered carbons and positive on the odd-numbered carbons, except C_5 which is slightly negative. An increase in the alternation of partial positive and negative charge differences on the odd and even-numbered carbon atoms, respectively, is observed with increased Schiff base-counterion distance. As the counterion is moved away from the PSB, partial positive charge that was stabilized on the imine proton migrates down the retinylidene chain, resulting in an increase of positive charge on the odd-numbered carbons. The charge density differences observed in rhodopsin are shown for comparison (*filled circles*) and serve to emphasize the positive change in charge density at C_8, C_{10}, and C_{12} and an anomalous negative change at C_5. Similar ^{13}C chemical shifts for C_5 and C_{12} were obtained by de Grip and coworkers (Mollevanger et al., 1987). These comparisons indicate that the rhodopsin chemical shifts cannot be modeled by simply moving the counterion away from the chromophore.

Charge densities were also calculated for models with a chloride counterion positioned along the retinal chain from C_{10} to C_{15}. The counterion is located out of the retinal plane with the $C_n \cdots Cl^-$ axis perpendicular to the plane defined by atoms C_{n-1}, C_n, and C_{n+1} and has been positioned at a series of distances (3.0 to 5.0 Å in 0.5-Å increments) from each conjugated carbon. Fig. 2 *b* presents the results for a counterion located 3.0 (*open circles*) and 5.0 Å (*open squares*) from C_{13}. In both cases, a general trend of alternating negative and positive character is seen with a large calculated difference between C_{13} and C_{12} (approximately 0.08 unit charge) in contrast to the moderate difference (0.02

unit charge) observed in the experimental data (*filled circles*). The simplest way to decrease the partial negative charge at C_{12} is to place the external negative charge closest to this position (Fig. 2 *c*, *open circles*). When compared to the calculated results for the counterion localized at C_{13}, placing the negative charge 3.0 Å above C_{12} results in an even distribution of charge differences on the retinal carbons which resembles the experimental data. This gave the best linear fit of all the chloride positions calculated in this series with a slope of 100 ppm/unit charge, a low intercept of 0.20 ppm and a high correlation coefficient ($R = 0.89$). The correlation coefficient drops to 0.82 when the distance is increased to 4.0 Å. Placing the charge 3.0 Å from C_{13} (Fig. 2 *b*, *open circles*) yielded a worse fit with a slope of 66 ppm/unit charge, an intercept of 0.70 ppm and an R of 0.81. All the other counterion locations modeled in this series gave correlation coefficients of less than 0.80.

A second series of charge densities were calculated for models having a chloride counterion positioned in the plane of the retinal both above and below the chromophore at 3.5–4.5 Å from C_{10} to C_{15}. These in-plane orientations consistently yielded poor calculated fits to the experimental data, except for those positions along the C_{12}-H bond. In order to constrain the angle of the $C_{12} \cdots Cl^-$ axis relative to the retinal plane, charge densities were also calculated for a series of orientations from −180° to 180° in 15° steps where 0° is defined as the in-plane orientation along the C_{12}-H bond. Acceptable fits to the NMR data were obtained for counterion orientations between approximately 90° and −45°.

The influence of a second negative charge in close proximity to the chromophore was addressed by calculating charge densities with one chloride counterion at 3.0 Å from C_{12} as in Fig. 2 *c* and a second charge located either 3.0–5.0 Å out of the retinal plane centered at C_{10} to C_{15} or in the retinal plane 3.25 Å from the SB nitrogen along the N-H bond (Fig. 2 *d*). Placing the second charge within 4.5 Å of the retinylidene chain invariably resulted in worse calculated fits to the experimental data than having a single charge at C_{12} alone. Poor calculated fits were also obtained for several additional two charge configurations, such as two chloride ions centered at C_{11} and C_{13} or at C_{13} and C_{15}. These results support the model of a neutral binding site in rhodopsin (Birge et al., 1985).

Finally, we tested the possibility that the anomalous downfield shift at C_{12} may alternatively arise from a change in the $C_{11}C_{12}C_{13}C_{14}$ torsion angle. Charge density calculations were carried out on the 11-*cis*-RPSB·Cl salt and the 11-*cis*-RPSB cation at torsion angles of 20° and 60°, bracketing the 40° angle used for the 11-*cis*-RPSB·Cl reference. Comparison of the charge distribution between the 20° and 60° geometries shows very little decrease in partial negative charge at C_{12} and the other even-numbered carbons (Fig. 3). In contrast, this large 40° change in torsion angle leads to a substantial gain or loss of partial positive charge at the odd-numbered carbons depending on their position relative to the Schiff base and the C-C twist. These results are expected

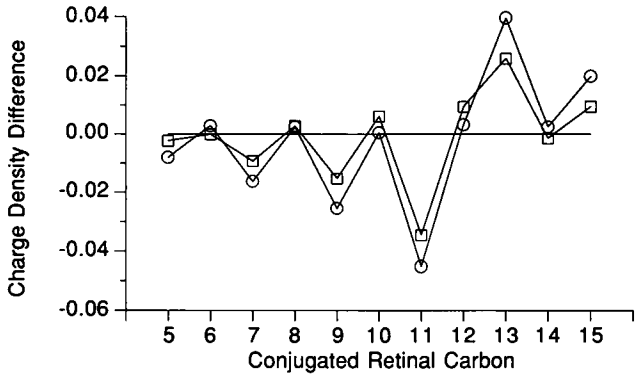

FIGURE 3 Effect of torsion angle on the charge distribution. The charge density difference between $C_{11}C_{12}C_{13}C_{14}$ torsion angles of 60° and 20° for 11-*cis*-RPSB (○) and 11-*cis*-RPSB·Cl (□).

when the conjugated system is broken and argue that the large downfield shift at C_{12} is not due to a change in torsion angle.

The major conclusion from the charge density calculations at this stage is that the unique pattern of partial charges along the retinylidene chain derived from the rhodopsin chemical shifts can be roughly modeled by placing a single charge 3.0 Å from C_{12} out of the retinal plane (Fig. 2 *c*). It is necessary to position the counterion *closest* to C_{12} in order to fit the large downfield C_{12} shift and, importantly, this placement reproduces the relatively smaller downfield shifts at the other even-numbered carbons (C_6, C_8, and C_{10}). It is worth noting that when the charge is 3.0 Å from C_{12}, as in the geometry defined above, it is also close to C_{11} (3.3 Å), C_{13} (3.3 Å), and C_{15} (4.2 Å), and the dominant electrostatic interactions are still between the counterion and the C_{13} and C_{15} carbons due to the large partial positive charges at these positions.

Since Glu^{113} has been shown to be the counterion in rhodopsin, a carboxylate ion (CH_3-COO^-) was used to model the binding site. The carboxylate group is a much more complex counterion than the chloride ion used above in having two oxygen atoms ~2.2 Å apart and bearing partial negative charges. The chloride ion results (Fig. 2), however, provide important insights into the possible locations and orientations of the carboxylate ion relative to the 11-*cis*-RPSB. Based on the calculations with two charges in the binding site, it is very unlikely that both oxygens of the carboxylate strongly interact with the retinal chain. Charge density differences for a series of CH_3-COO^- orientations have been calculated with one oxygen atom (O_1) fixed at 3.0 Å from C_{12} in the same position as the chloride counterion in Fig. 2 *c*. The carboxylate group was then rotated to place the second oxygen (O_2) in different positions in an arc from C_{10} to C_{14} as well as near the Schiff base proton. The best fit corresponded to the orientation shown in Fig. 4 *c*, which has one oxygen 3.0 Å from C_{12} out of the retinal plane (as in Fig. 2 *c*) and the other one pointing away from the chain, consistent with the results using chloride counterions. The calculated fit is also better than in the single charge case in all parameters (Fig. 4, *a* and *b*) due to the weaker electrostatic interaction from the *partial*

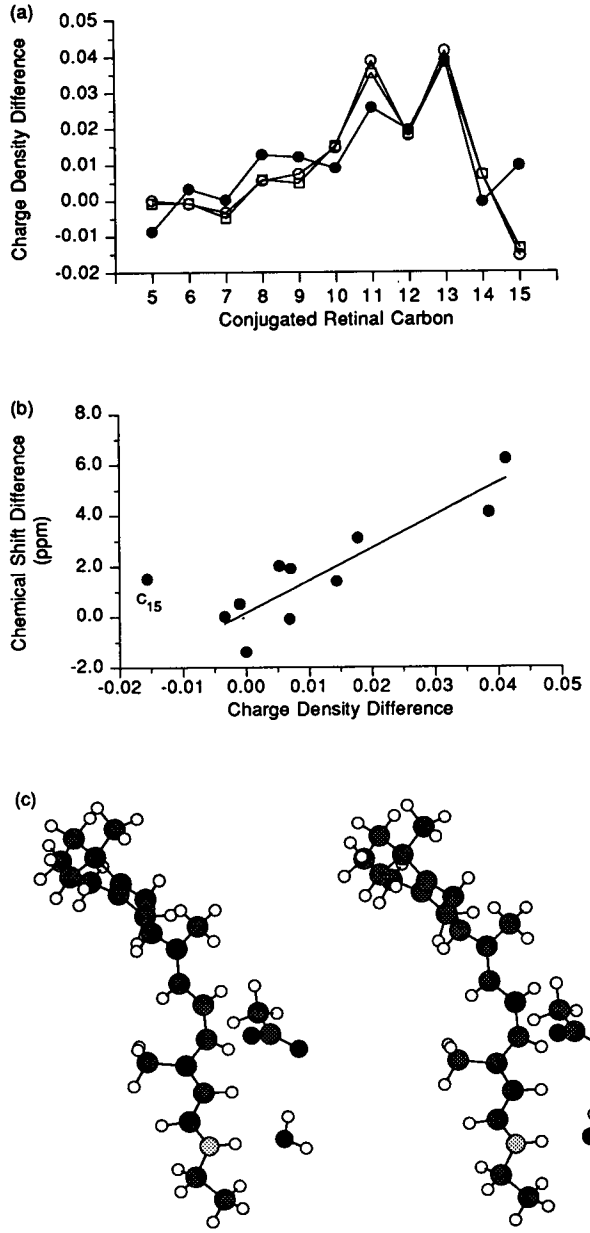

FIGURE 4 Modeling the retinal binding site of rhodopsin with a CH_3-COO^- counterion at C_{12} and water hydrogen-bonded to the Schiff base proton. (*a*) Comparison of charge density differences of the experimental data (●) with models having a CH_3-COO^- counterion alone (○) or a CH_3-COO^- counterion and H_2O (□). (*b*) Correlation of the NMR data with the calculated charge density difference for the binding site model having a CH_3-COO^- counterion. The calculated fit has a slope of 128 ppm/unit charge, an intercept 0.14 ppm and an R of 0.90. When water is included the calculated fit has a slope of 135 ppm/unit charge, an intercept of 0.18 ppm and an R of 0.90. C_{15} is excluded in these fits. (*c*) Stereo view of the binding site model with a CH_3-COO^- counterion and H_2O. The key distances are $C_{12}\cdots O_1$ (CH_3-COO^-) 3.0 Å, $C_{12}\cdots O_2$ (CH_3-COO^-) 5.1 Å, N-H$\cdots O_3$ (H_2O) 2.9 Å.

charge on the carboxylate oxygen. Attempts to bring the second oxygen to within 3.0 Å of another conjugated carbon (such as C_{10} or C_{14}) or the Schiff base proton disrupts the pattern in the same fashion as placing two chloride ions at the corresponding positions.

Fig. 4 *c* presents a stereo model with a CH_3-COO^- group at C_{12} and a water molecule with its oxygen (O_3) at optimal hydrogen bonding distance from the imine proton ($O_3 \cdots$ H-N, 2.9 Å), and its O-H bond oriented toward O_2 of the CH_3-COO^- counterion (O_2H-$O_3 \cdots$, 3.9 Å). Although the existence of water in the binding site cannot be directly derived from the NMR data, an H_2O molecule has been incorporated into the model in order to account for observations from other studies (see Discussion). The calculated charge densities with water in the binding site and with the carboxylate counterion alone exhibit equally good fits to the experimental data (Fig. 4 *a*).

DISCUSSION

There has been considerable interest in establishing the nature and location of charged residues interacting with the retinylidene chromophore in rhodopsin (see Birge (1990) for a review). Recent studies using site-directed mutagenesis have shown that Glu^{113} is responsible for a large red-shift in the absorption spectrum of the chromophore and may be involved in the mechanism of protein activation (Zhukovsky and Oprian, 1989; Sakmar et al., 1989; Nathans, 1990). In this study, we combine semiempirical calculations and NMR chemical shift data to argue for a strong interaction, presumably due to Glu^{113}, centered at C_{12} of the retinylidene PSB. The absorption studies using dihydroretinal derivatives were the first experimental evidence for a charge near C_{12} (Honig et al., 1979). Subsequent Raman studies have shown that there is a strong perturbation in *bathorhodopsin* that uncouples the C_{11}H-C_{12}H out-of-plane wagging vibration (Eyring et al., 1982; Palings et al., 1989), and that decreases when Glu^{113} is mutated to Gln or Ala (Lin et al., 1992). However, this mode is not influenced by the protein in rhodopsin. The presence of a negative protein charge near C_{12} in bathorhodopsin is consistent with the NMR observation of a large downfield shift of the C_{12} resonance in this intermediate (Smith et al., 1991). One possibility for the difference between the NMR and vibrational results in rhodopsin is that the vibrational coupling of the C_{11}H-C_{12}H mode is more sensitive to the detailed orientation of the carboxylate charge than the NMR chemical shift.

The model presented in Fig. 4 *c* is similar in many respects to that proposed by Birge and coworkers (Birge, 1990) based on absorption and vibrational studies. Both models argue for a neutral binding site with a carboxylate counterion having strong electrostatic interactions with the retinal chromophore at C_{13} and C_{15}, and not hydrogen-bonded to the Schiff base proton. The critical difference is in the position of the partial negative charges of the counterion along the retinylidene chain. In the previous model, both oxygen atoms from the carboxylate group interact with the chromophore, although only a single oxygen is constrained to lie within 4 Å of the C_{13}-C_{15} atoms in order to fit the observed transition energy and oscillator strength (Birge, 1990). Consequently, the counterion position cannot be uniquely defined. The NMR data indicates that only one of the oxygens interacts strongly

with the RPSB and that it *must* be closest to C_{12}. This rules out the close approach of the second oxygen to the retinal chromophore and constrains the location and orientation of the counterion within the range of positions previously allowed.

Finally, in order to account for the high C=N stretching frequency (~1660 cm^{-1}) and large ND isotope shift (~30 cm^{-1}) which indicate that the SB is strongly hydrogen-bonded (Mathies et al., 1976; Narva and Callender, 1980; Bagley et al., 1985; Baasov et al. 1987; Rodman Gilson et al., 1988), possibly to water in the binding site (Rafferty and Shichi, 1981; Cossette and Vocelle, 1987; Tallent et al., 1992), we have included water in the final calculations. It is of interest to note that this highly polar molecule has a much weaker influence on the calculated charge densities than a formal charge, suggesting that additional neutral polar residues can be incorporated into the binding site model. However, as pointed out by Tallent et al. (1992), additional effort still must be made to parameterize hydrogen-bonding interactions in order to accurately model the influence of water on the calculated charge densities. Further refinement of the distance and orientation of the carboxylate side chain relative to C_{12} is in progress that combines both the observed NMR and absorption data. These studies can be extended to localize protein-chromophore interactions in each of the rhodopsin photointermediates.

We gratefully acknowledge Professor Michael Zerner for a copy of the ZINDO program, and Professor Johan Lugtenburg for providing the 11-*cis*-retinals and catalyzing the NMR studies on rhodopsin. We thank Professor Robert Birge, Dr. Temple Burling, Dr. Günther Metz, Olve Peersen, and Peter Klosterman for helpful comments and discussion.

This work was supported by grant GM 41412 from the National Institutes of Health.

REFERENCES

Albeck, A., N. Livnah, H. Gottlieb, and M. Sheves. 1992. ^{13}C NMR studies of model compounds for bacteriorhodopsin: factors affecting the retinal chromophore chemical shifts and absorption maximum. *J. Am. Chem. Soc.* 114:2400–2411.

Baasov, T., N. Friedman, and M. Sheves. 1987. Factors affecting the C=N stretching in protonated retinal Schiff base: a model study for bacteriorhodopsin and visual pigments. *Biochemistry.* 26:3210–3217.

Bagley, K., V. Balogh-Nair, A. A. Croteau, G. Dollinger, T. G. Ebrey, L. Eisenstein, M. K. Hong, K. Nakanishi, and J. Vittitow. 1985. Fourier-transform infrared difference spectroscopy of rhodopsin and its photoproducts at low temperature. *Biochemistry.* 24:6055–6071.

Birge, R. R. 1990. Nature of the primary photochemical events in rhodopsin and bacteriorhodopsin. *Biochim. Biophys. Acta.* 1016:293–327.

Birge, R. R., L. P. Murray, B. M. Pierce, H. Akita, V. Balogh-Nair, L. A. Findsen, and K. Nakanishi. 1985. Two-photon spectroscopy of locked-11-*cis*-rhodopsin: evidence for a protonated Schiff base in a neutral protein binding site. *Proc. Natl. Acad. Sci. USA.* 82:4117–4121.

Birge, R. R., C. M. Einterz, H. M. Knapp, and L. P. Murray. 1988. The nature of the primary photochemical events in rhodopsin and isorhodopsin. *Biophys. J.* 53:367–385.

Blatz, P. E., J. H. Mohler, and H. V. Navangul. 1972. Anion-induced wavelength regulation of absorption maxima of Schiff bases of retinal. *Biochemistry.* 11:848–855.

Cossette, D., and D. Vocelle. 1987. A ^{13}C and ^{15}N nuclear magnetic resonance study of the protonation of a retinal Schiff base by acids of different pK_as and in solvents of different polarities. *Can. J. Chem.* 65: 1576–1583.

Eyring, G., B. Curry, A. Broek, J. Lugtenburg, and R. Mathies. 1982. Assignment and interpretation of hydrogen out-of-plane vibrations in the resonance Raman spectra of rhodopsin and bathorhodopsin. *Biochemistry.* 21: 384–393.

Gilardi, R. D., I. L. Karle, and J. Karle. 1972. The crystal and molecular structure of 11-*cis* retinal. *Acta Cryst. Sci.* B28:2605–2612.

Harbison, G. S., P. P. J. Mulder, H. Pardoen, J. Lugtenburg, J. Herzfeld, and R. G. Griffin. 1985. High-resolution carbon-13 NMR of retinal derivatives in the solid state. *J. Am. Chem. Soc.* 107:4809–4816.

Honig, B., and M. Karplus. 1971. Implications of torsional potential of retinal isomers for visual excitation. *Nature (Lond.).* 229:558–560.

Honig, B., A. D. Greenberg, U. Dinur, and T. G. Ebrey. 1976. Visual-pigment spectra: implications of the protonation of the retinal Schiff base. *Biochemistry.* 15:4593–4599.

Honig, B., U. Dinur, K. Nakanishi, V. Balogh-Nair, M. Gawinowicz, M. Arnaboldi, and M. G. Motto. 1979. An external point-charge model for wavelength regulation in visual pigments. *J. Am. Chem. Soc.* 101:7084–7086.

Inoue, Y., Y. Tokito, R. Chujo, and Y. Miyoshi. 1977. A study of π-electron delocalization in model compounds of visual pigment by UV and carbon-13 NMR spectra. *J. Am. Chem. Soc.* 99:5592–5596.

Kropf, A., and R. Hubbard. 1958. The mechanism of bleaching rhodopsin. *Ann. NY Acad. Sci.* 74:266–280.

Lauterbur, P. 1961. ^{13}C nuclear magnetic resonance spectroscopy. I. Aromatic hydrocarbons. *J. Am. Chem. Soc.* 83:1838–1846.

Lin, S. W., T. P. Sakmar, R. R. Franke, H. G. Khorana, and R. A. Mathies. 1992. Resonance Raman microprobe spectroscopy of rhodopsin mutants: effect of substitutions in the third transmembrane helix. *Biochemistry.* 31:5105–5111.

Mathies, R., A. R. Oseroff, and L. Stryer. 1976. Rapid-flow resonance Raman spectroscopy of photolabile molecules: rhodopsin and isorhodopsin. *Proc. Natl. Acad. Sci. USA.* 73:1–5.

Mollevanger, L. C. P. J., A. P. M. Kentgens, J. A. Pardoen, J. M. L. Courtin, W. S. Veeman, J. Lugtenburg, and W. J. de Grip. 1987. High-resolution solid-state ^{13}C NMR study of carbon C-5 and C-12 of the chromophore of bovine rhodopsin. *Eur. J. Biochem.* 163:9–14.

Narva, D., and R. H. Callender. 1980. On the state of chromophore protonation in rhodopsin: implication for primary photochemistry in visual pigments. *Photochem. Photobiol.* 32:273–276.

Nathans, J. 1990. Determination of visual pigment absorbance: identification of the retinylidene Schiff's base counterion in bovine rhodopsin. *Biochemistry.* 29:9746–9752.

Nathans, J. 1992. Rhodopsin: structure, function and genetics. *Biochemistry.* 31:4923–4931.

Palings, I., E. M. M. van den Berg, J. Lugtenburg, and R. A. Mathies. 1989. Complete assignment of the hydrogen out-of-plane wagging vibrations of bathorhodopsin. *Biochemistry.* 28:1498–1507.

Rafferty, C. N., and H. Shichi. 1981. The involvement of water at the retinal binding site in rhodopsin and early light-induced intramolecular proton transfer. *Photochem. Photobiol.* 33:229–234.

Rodman Gilson, H. S., and B. H. Honig. 1988. Analysis of NMR and absorption spectroscopic data in bacteriorhodopsin: models for protein-chromophore interactions. *J. Am. Chem. Soc.* 110:1943–1950.

Rodman Gilson, H. S., B. Honig, A. Croteau, G. Zarrilli, and K. Nakanishi. 1988. Analysis of the factors that influence the C=N stretching frequency of polyene Schiff bases. *Biophys. J.* 53:261–269.

Sakmar, T. P., R. R. Franke, and H. G. Khorana. 1989. Glutamic acid-113 serves as the retinylidene Schiff base counterion in bovine rhodopsin. *Proc. Natl. Acad. Sci. USA.* 86:8309–8313.

Sanders, G. M., M. van Dijk, H. C. van der Plas, M. Konijn, and C. H. Stam. 1983. Reactions of halogenoquinolizinium bromides with aniline, isopropylamine and liquid ammonia. *J. Heterocycl. Chem.* 20:407–414.

Shriver, J., E. W. Abrahamson, and G. D. Mateescu. 1976. The structure of visual pigments. I. Carbon-13 nuclear magnetic resonance spectroscopy of N-all-*trans*-retinylidenepropylimine and its protonated species. *J. Am. Chem. Soc.* 98:2407–2409.

Shriver, J. W., G. D. Mateescu, and E. W. Abrahamson. 1979. A proton and carbon-13 nuclear magnetic resonance spectroscopy study of the conformation of a protonated 11-*cis*-retinal Schiff base. *Biochemistry.* 18: 4785–4792.

Smith, S. O., I. Palings, M. E. Miley, J. Courtin, H. de Groot, J. Lugtenburg,

R. A. Mathies, and R. G. Griffin. 1990. Solid-state NMR studies of the mechanism of the opsin shift in the visual pigment rhodopsin. *Biochemistry.* 29:8158–8164.

Smith, S. O., J. Courtin, H. de Groot, R. Gebhard, and J. Lugtenburg. 1991. ^{13}C Magic-angle spinning NMR studies of bathorhodopsin, the primary photoproduct of rhodopsin. *Biochemistry.* 30:7409–7415.

Spiesecke, H., and W. G. Schneider. 1961. The determination of π-electron densities in azulene from ^{13}C and ^{1}H nuclear resonance shifts. *Tetrahedron Lett.* 14:468–472.

Tallent, J. R., E. W. Hyde, L. A. Findsen, G. C. Fox, and R. R. Birge. 1992. Molecular dynamics of the primary photochemical event in rhodopsin. *J. Am. Chem. Soc.* 114:1581–1592.

Tavan, P., K. Schulten, and D. Oesterhelt. 1985. The effect of protonation and electrical interactions on the stereochemistry of retinal Schiff bases. *Biophys. J.* 47:415–430.

Tokuhiro, T., and G. Fraenkel. 1969. Origin of linearity of carbon-13 shift with charge. Calculations for the azines. *J. Am. Chem. Soc.* 91:5005–5013.

Warshel, A., and M. Karplus. 1974. Calculation of $\pi\pi^*$ excited state conformations and vibronic structure of retinal and related molecules. *J. Am. Chem. Soc.* 96:5677–5689.

Zelnik, R., M. Haraguchi, A. K. Matida, D. Lavie, F. Frolow, and A. L. Weis. 1986. X-ray molecular structure of caissarone, a novel purine derivative from the sea anemone *Bunodosoma caissarum* Correa 1964. *J. Chem. Soc. Perkin Trans. I.* 2051–2053.

Zhukovsky, E. A., and D. D. Oprian. 1989. Effect of carboxylic acid side chains on the absorption maximum of visual pigments. *Science (Wash. DC).* 246:928–930.